# Evaluation of the binding energy of viral capsid proteins using a Virtual AFM

Sergi Roca Bonet
*Departament de Física de la Matèria Condensada, Facultat de Física, Universitat de Barcelona, Diagonal 645, 08028 Barcelona, Spain.**

Advisor: Prof. David Reguera López

**Abstract:** Viruses are biological agents with great potential in the field of nanotechnology. Nowadays, their amazing properties are starting to be unveiled using physical techniques like the atomic force microscope. In this study, we have used a Virtual AFM, i.e., a simulator that mimics a typical AFM nanoindentation experiment, to study the mechanical properties of viral shells. In particular, with our VAFM, we have analysed the possibility of evaluating the binding energy between proteins using rupture experiments and how that estimate of the energy depends on experimental parameters such as the loading rate or the size of the tip.

## I. INTRODUCTION

Viruses are infectious agents that replicate their genetic material inside living cells, and are not capable of any other metabolic activity. Their most remarkable impact in our daily lives is dominated by their role as vectors of serious and minor diseases. But viruses are starting to be used for promising applications such as batteries and memory devices, as nanoscaffolds or nanoreactors, or as vectors for gene therapy.

In their simplest form, viruses are made by a protein shell, or capsid, which protects their genetic material, typically a highly-compacted RNA or DNA chain. Viral capsids are usually a one-protein-thick shell made by several copies of a protein, that self-assembles spontaneously [1, 3, 4]. The resulting capsid is in most cases quasispherical with icosahedral symmetry and can be classified in terms of the triangulation number T. A T-number virus has 60T proteins, organized in 12 *pentamers* and 10(T-1) *hexamers*, which are clusters of five or six proteins, respectively.

The development of new techniques, and in particular, of AFM, has helped the study of the mechanical properties of individual viruses. An AFM consists of a sharp tip attached to the end of a microcantilever, which is approached to the surface of an object, e.g., the virus, by means of a piezoelectric device. AFM is typically used to obtain a topographic map of the sample, but it also provides useful information about its mechanical properties. In order to understand and to interpret experiments, modelling and theoretical understanding are crucial.

Beyond the mechanical properties of viruses, there is interest in obtaining the energy that keeps the viral shell proteins bound. Some experimental studies are probing the possibility of estimating this energy using an AFM. In particular, recent indentation experiments using adenovirus, [2], have been able to induce the breaking of the shell by the release of a single hexamer. This breaking event can be detected by an irreversible change in the force-indentation curves, allowing to give an estimate of the binding energy of these capsomers.

In this study, we will analyse the possibility of obtaining the binding energy between proteins by simulating these rupture experiments with a VAFM. Moreover, we will try to determine how this estimation of the energy depends on external parameters such as the loading rate or the size of the tip of the cantilever.

## II. VIRTUAL ATOMIC FORCE MICROSCOPE

In order to study the mechanical properties of viral nanocages, we have used a VAFM, i.e., a simulation that aims to imitate the nanoindentation experiments performed by an AFM.

We have used a coarse-grained model since it is almost impossible to describe these experiments with atomistic detail.

Our model is coarse-grained at the level of capsomers, i.e., pentamers and hexamers, which are the basic structural units of a viral shell. These capsomers are represented as effective spheres of two different sizes: $\sigma_h$ and $\sigma_p = 0.8\sigma_h$, reflecting the fact that pentamers and hexamers are made of a different number of proteins (five and six, see Figure 1).

The interaction between capsomers is modelled using three contributions: a Lennard-Jones, an angular and a torsion potential, $V = V_{LJ} \cdot V_a \cdot V_{tor}$. The Lennard-Jones potential describes the binding and the excluded volume interaction between a pair of capsomers in terms of the relative distance, $\mathbf{r}_{ij}$. The expression used has been [1]

$$V_{LJ}(\mathbf{r}_{ij}) = \epsilon_{ij}\left[\left(\frac{\sigma_{ij}}{r}\right)^{12} - 2\left(\frac{\sigma_{ij}}{r}\right)^{6}\right], \qquad (1)$$

where $\sigma_{ij}$ is the equilibrium distance corresponding to the minimum of the potential, $r$ is the distance between capsomers centres, and $\epsilon_{ij}$ is the binding energy between capsomers.

*Electronic address: sergi.rb94@gmail.com

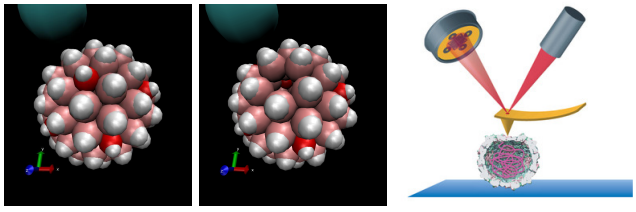

**(a)** **(b)** **(c)**

**Figure 1:** Visual representation of the viral nanocage using the coarse-grain model (a) before indentation, (b) after the removal of the pentamer and (c) a comparison with a real AFM. Pentamers, hexamers and the tip of the cantilever are represented by red, pink and a big blue sphere, respectively, on figures (a) and (b). Both images (a) and (b) were obtained from the simulation using VMD and (c) from [9].

The angular term of the potential is given by [1]

$$V_a(\mathbf{r}_{ij}, \mathbf{\Omega}_i, \mathbf{\Omega}_j) = \exp\left(-\frac{(\theta_{ij}-\nu)^2}{2\alpha^2}\right)\exp\left(-\frac{(\theta_{ji}-\nu)^2}{2\alpha^2}\right), \tag{2}$$

where $\theta_{ij}$ is the angle between the vector $\mathbf{\Omega}_i$ describing the spatial orientation of the capsomer, and the unit vector $\mathbf{r}_{ij}$. The parameter $\nu$ is the preferred angle, related to the spontaneous curvature, which defines the size of the shell, and the parameter $\alpha$ controls the local bending stiffness.

Finally, the last contribution to the potential is the torsion term, included to favour the formation of closed shells instead of connected surfaces with different concavity. This contribution is given by [1]

$$V_{tor}(\mathbf{\Omega}_i, \mathbf{\Omega}_j) = \exp\left(-k_t\frac{(1-\cos\xi)}{2}\right), \tag{3}$$

where $k_t$ is the torsion constant and $\xi$ is the angle between the planes defined by the unit vector $\mathbf{r}_{ij}$ and both orientation vectors.

This model has been implemented in a Brownian Dynamics simulation code.

The integration algorithm used was stochastic Euler's. This algorithm gives the position of the capsomers at a time t+$\Delta$t,

$$r_k(t+\Delta t) = r_k(t) + \frac{F_k(t)\Delta t}{\eta} + \sqrt{2D\Delta t}\,\xi_k, \tag{4}$$

where $\eta$ is the friction coefficient, $\xi_k$ is a Gaussian white noise number and $D$ is the diffusion coefficient [1].

Our VAFM is a simulation that emulates the indentation process of an AFM, i.e., simulates the lowering of a spherical tip of radius $R_t$ attached to a microcantilever which punctures our sample, in this case, an empty T=7 viral nanocage.

In the immobilized simulation, the virus is on the substrate, by fixing the position of the lowest hexamers. Initially, the spherical tip is placed at a height $h$ above the sample, and the average energy of the viral shell without indentation and the potential energy of the top pentamer are obtained.

The simulation is then run for a total of typically $10^6$ timesteps, with $\Delta t = 10^{-5}\tau$. The tip of the cantilever is lowered at steps of $\Delta h = 5\cdot 10^{-3}\sigma$. The average force between the tip and the virus is evaluated as a function of the indentation.

We worked using reduced units in terms of the diameter of the hexamers as a measure of longitudes, $\sigma$, which takes the value of 12.5 nm; the characteristic diffusion time of the capsomers, $\tau = \sigma^2/D$, obtained using the Stokes-Einstein equation for hexamers diluted in water, which for our subunits corresponds to 4 $\mu$s; and the binding energy between hexamers, $\varepsilon_0 = 20k_BT$.

In these reduced units, the parameters used in the simulation are: the binding stiffness, $\alpha = 1$, the preferred angles between capsomers, $\nu = 1.796$ and the torsion constant, $k_t = 1.5$.

## III. KRAMERS-BELL THEORY

In this study we will monitor the failure of the pentamer on top of the nanocage, i.e., the breaking of the bonds between that capsomer and its neighbours. Bond-breaking is usually interpreted in terms of Kramers-Bell theory, since it can be represented as the transition between two states: bound and unbound pentamer.

Kramers theory describes bond breaking in the absence of external forces as a escape from a deep energy minimum (i.e., bound state) jumping over a barrier, whose maximum defines the transition state. The transition rate between states is proportional to the exponential of the barrier's height, $k_{\rightarrow} \propto \exp(-E_b(f)/k_BT)$ [5]. Thus, it will be possible to assign an intrinsic lifetime to the bound state, $\tau_0 = 1/k_{\rightarrow}$ [6].

If we apply and external force, the barrier height decreases, increasing the transition rate and decreasing the lifetime of the initial state, making more probable to jump from bound to transition state [5, 6]. Bell's phenomenological expression describes the lifetime of the bound state as a function of the applied force and the intrinsic lifetime, $\tau_{Bell} = \tau_0\exp(-\beta F x^{\ddagger}) < \tau_0$, where $x^{\ddagger}$ is the distance to the transition state, and $\beta^{-1} \equiv k_BT$.

It has also been demonstrated that the loading rate has a critical effect on the bond strength. The bond strength, $f^*$, i.e., in our case, the maximum force that the pentamer can hold, is expected to have a logarithmic dependence with the loading rate, $\Delta f/\Delta t$. The exact slope is set by the thermal force, $f^* = f_\beta \ln(r_f)$ [5], where $f_\beta = k_BT/x^{\ddagger}$, and $r_f = (t_{off}k_f v)/f_\beta$. Thus, by measuring the breaking force as a function of the natural logarithm of the loading rate and making a linear regression, it is possible to estimate the indentation $x^{\ddagger}$ corresponding to the transition state. Extrapolating this regression to zero force, the lifetime of that state, defined as $t_{off} = f_\beta/(\Delta f/\Delta t)_{f=0}$ can be obtained [5].

## IV. RESULTS

Using the VAFM, we have studied the mechanical response of a T=7 capsid during an indentation process. By analysing the indentation curves, we are going to find out the behaviour of the maximum force and indentation that the virus can hold before losing the top pentamer, as a function of the loading rate and the radius of the cantilever's tip. We are also going to show that the integration of these curves give a reasonable estimation of the value of the binding energy between capsomers.

### A. Force-indentation curves

The mechanical properties of viruses are typically obtained from force-indentation curves (Figure 2). A force-indentation curve shows the dependency of the force applied by the tip of the VAFM to the virus with the indentation, i.e., the variation in height of the viral nanocage with respect the height of the undeformed capsid. These curves were obtained by lowering the tip up to a maximum indentation, followed by the retraction of the tip.

From these force-indentation curves, the elastic constant, the breaking force and the maximum indentation can be obtained. The jump represents the release of the top pentamer. If there's no rupture, the curve is reversible when the tip is retracted. If the virus suffers some rupture, the curve is no longer reversible, and a hysteresis cycle appears. By integrating the area inside the curve it is possible to obtain the dissipated energy.

As it can be seen on Figure 2, the spring constant of the nanocage, i.e., the slope of the force-indentation curves, does not depend on the radius of the tip of the cantilever. Nonetheless, the breaking force and maximum indentation before the rupture indeed depend on the tip radius.

After shell breaking, the spring constant associated with the retraction of the tip, depends on the tip radius. That can be explained using the theory of elasticity for spherical shells [8]. In essence, it is due to the fact that, unlike closed shells, when the shell loses a pentamer, it has a hole in it. Then, it can be indented without suffering any stretching.

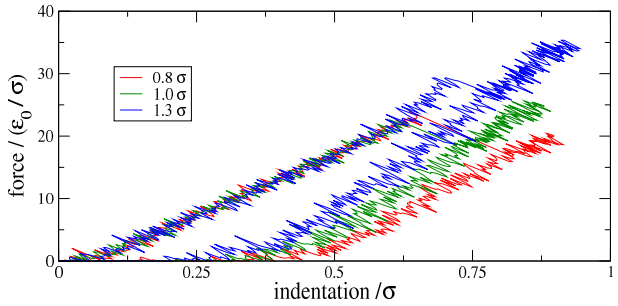


**Figure 2:** Indentation curves showing the forward and reverse trajectories for different radius of the tip, indicated in the legend.

### B. Loading Dynamics

An important part of this project is to study the dependency of the breaking force with the loading rate to check if it agrees with Kramers-Bell theory. Indeed, our results show that the force at which the pentamer gets unbound show a linear dependency with the logarithm of the loading rate. This dependency is clearly shown on Figure 3, where we represented these parameters for a tip of radius $0.8\sigma$. Our results differ from the experimental study made by Snijder et al, [7], who did not obtained that logarithmic relation, in contradiction with the theory.

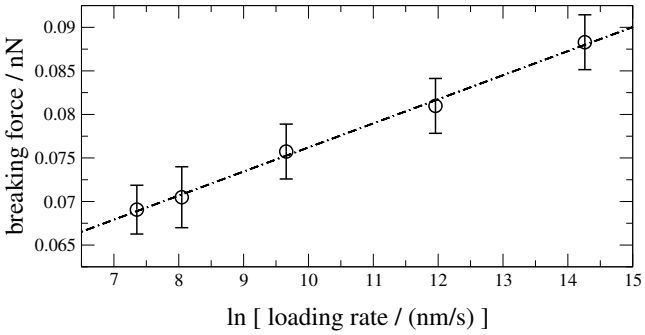


**Figure 3:** Representation of the logarithmic dependency of the breaking force with the loading rate for a tip of radius $0.8\sigma$, expressed in real units.

Our range of loading rates encompasses the ones from [7] given that they worked in a range of velocities from 6 to 6000 nm/s, whilst the range of our loading rates range from 1600 to 1600000 nm/s. Our smaller loading rates coincide with their maximum value of that same parameter. Our smallest loading rate is one order of magnitude larger than the experimental one from [2], which was of 150 nm/s.

From Figure 3, we have also obtained the value of the indentation corresponding to the transition state, obtaining a value of $z_\beta = 0.12 \pm 0.05\sigma$. This value is one order of magnitude smaller than the inflection point of the Lennard-Jones potential, located at $r^* = 1.1\sigma$ for our potential. That can be due to the fact that we are not stretching two capsomers radially.

Also, from the linear regression of Figure 3, we were able to find out the intrinsic lifetime of the viral capsid when no external force is applied. We obtained a lifetime of $t_{off} \sim 10^7$s, allowing us to assume that the viral nanocage with all its pentamers is a very stable structure.

### C. Breaking Force and Maximum Indentation

We have studied the behaviour of the breaking force and the maximum indentation as a function of both the loading rate and the size of the cantilever's tip (see Figure 4). We have obtained that both the breaking force

and the maximum indentation increase with the radius of the tip. When performing indentations with tips of radius larger than $1.8\sigma$, not only the pentamer gets sunk, but its surrounding hexamers too. That leads to greater resistances of the shell given the larger amount of bonds involved in the indentation.

The breaking force increases with the loading rate, as it was expected. Given that the spring constant results from the ratio of the force and the indentation, and since it remains constant regardless of the size of the tip, the maximum indentation must show the same behaviour as the breaking force, as shown on the last plot of Figure 4. Nevertheless, the values of the maximum indentation at finite loading rates differ from the value of the transition indentation, $z_\beta$, found using the relation between the breaking force and the loading rate within the framework of Kramers-Bell theory.

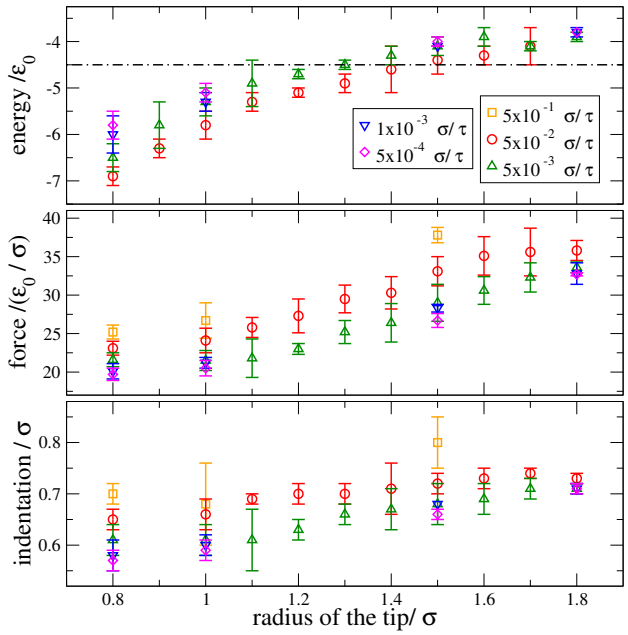


**Figure 4:** Behaviour of the energy released due to the failure of the pentamer, the breaking force and the maximum indentation as a function of both the size of the tip and the loading rate. The discontinuous line on the energy plot represents the expected value of the pentamer's energy, $\mathcal{U}^* = -4.5\varepsilon_0$.

### D. Effective Binding Energy of the pentamer

In this section, we have calculated the effective binding energy of the pentamer using three different methods. First of all, we estimated the average potential energy expected for every capsomer using the total potential energy of the viral nanocage and the number of bonds on the structure. The total energy of the shell before the indentation was evaluated from the simulation, obtaining an average value of $\mathcal{U} = -190\pm1\varepsilon_0$. Knowing then that the total number of bonds is $\#_b$=210, the energy released by the loss of one pentamer can be calculated as $\mathcal{U}^* = \frac{5}{\#_b}\mathcal{U} = -4.5\varepsilon_0$.

Another way of obtaining an estimation of that energy has been to calculate the potential energy of the pentamer before the tip interacts with the structure, i.e., only as a result of the interaction between the pentamer and the surrounding hexamers. By averaging over several simulations, the value of that energy has been found to be $\mathcal{U}^* \sim -4.5\pm0.5\varepsilon_0$.

The last method for calculating the energy was to evaluate the area of the hysteresis cycle of the force-indentation curves by integrating these curves. Using that method, we found that the energy released by the failure of the pentamer has a strong dependency on both the radius of the tip and the loading rate, as it can be seen on Figure 4.

The fact that the binding energy between the pentamer and the surrounding hexamers depends on the radius of the tip can be due to a geometric effect especially important for small tips. When the pentamer gets dissassemblied, the tip falls partially inside the shell, causing to measure a greater fall on the force-indentation curves resulting on an overestimation of that area. This effect is enhanced for small tip, whilst for sufficiently large tips, that effect of the indentation can be neglected, causing the saturation observed on the first plot of Figure 4.

### E. Strength of the Binding Energy between H-P

This final part of our study was focused on determining whether the measured effective binding energy of a pentamer measured from the hysteresis cycle was indeed proportional to $\varepsilon_{hp}$, i..e, the binding energy between hexamer and pentamer in the model. The results plotted in Figure 5 for $R_t$=1$\sigma$ confirm this linear relationship. From the linear regression of Figure 5, we have obtained that the binding energy of the pentamer increases as $\mathcal{U}^* = -6.7\varepsilon_{hp} + 1.0$. As it was expected, the average binding energy of the pentamer is proportional to the binding energy between hexamer-pentamer, $\varepsilon_{hp}$. Nevertheless, this value of the energy is overestimated, possibly as a result of the effect of the size of the tip and the loading rate.

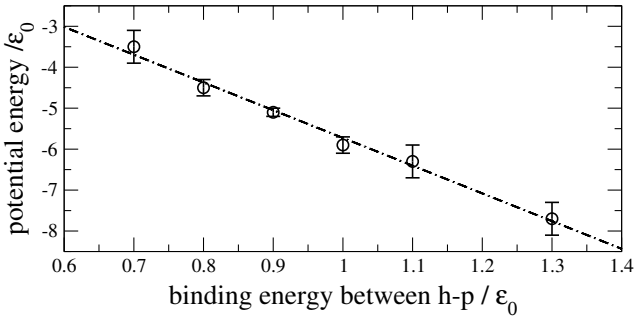


**Figure 5:** Behaviour of the effective binding energy of the pentamer as a function of the binding energy between an hexamer and a pentamer in the model, $\varepsilon_{hp}$.

## V. CONCLUSIONS

This study had the objective of exploring the possibility of obtaining an accurate estimation of the binding energy between capsomers using an AFM nanoindentation experiments.

We have shown that, unlike the spring constant, the breaking force and the maximum indentation depend on both the loading rate and the radius of the cantilever's tip. Both properties are overestimated at higher loading rates and large tip radius.

Finally, we found that it is possible to obtain a reasonable estimate of the value of the binding energy between proteins of a viral nanocage by using an AFM. However, the values obtained depend on both the loading rate and the tip radius, and tend to be overestimated.

Our study opens the door to use this method in real AFM experiments. It would be interesting to determine experimentally approximate values for other viruses, which may be correlated with estimated values found using other methods, such as calorimetry.

### Acknowledgments

I would like to special thank my advisor, Prof. David Reguera, for his support, patience and guidance through this work, and also really thank him for the opportunity he has given me to collaborate in this project. Also, thanks to my friends and family, who had to endure my monologues about puncturing viruses.

[1] M. Aznar, *Coarse-Grained Modeling of the Assembly and Mechanical Properties of Viruses*, Ph.D. Thesis, Universitat de Barcelona, 2013.

[2] A. Ortega-Esteban, *Biophysical determinants for adenovirus uncoating and inefectivity*, Ph.D. Thesis, Universidad Autónoma de Madrid, 2015.

[3] A. Luque, D. Reguera, *Theoretical studies of assembly, physical stability and dynamics of viruses*, in "Structure and Physics of Viruses", M. G. Mateu (Ed.), Springer, Netherlands, 2013.

[4] W. H. Roos, R. Bruinsma, G. J. L. Wuite, *Physical Virology*, Nature Physics, 6, 733-743, 2010.

[5] E. Evans, *Probing the relation between force-lifetime-and Chemistry in single molecular bonds*, Annu. Rev. Biophys. Struct. 30,105-128, 2001.

[6] O. K. Dudko, G. Hummer, A. Szabo, *Theory, analysis, and interpretation of single-molecule force spectroscopy experiments*, PNAS, 105, 15755-15760, 2008.

[7] J. Snijder, I. L. Ivanovska, M. Baclayon, W. H. Roos, G. J. L. Wuite, *Probing the impact of loading rate on the mechanical properties of viral nanoparticles*, Micron 43, 1343-1350, 2012.

[8] L. D. Landau, E. M. Lifshitz, *Theory of elasticity*, Pergamon Press, 1970.

[9] *Untangling heterogeneous populations of a virus with mass spectrometry (MS) and atomic force microscopy (AFM)* , [online]: `http://www.nature.com/nchem/journal/v5/n6/figtab/nchem.1666F1.html`